

Cheng Yuan<sup>\*†</sup>, William K. M. Lau<sup>†#</sup>, Zhanqing Li<sup>†#</sup>

<sup>\*</sup>School of Atmospheric Science, Nanjing University <sup>#</sup>Department of Atmospheric and Oceanic Science, University of Maryland

<sup>†</sup>Earth System Science Interdisciplinary Center, University of Maryland.

**Background:** The Asian Tropopause Aerosol Layer (ATAL), recently discovered from satellite observations, has drawn much attention on the need to study and better understand processes of atmospheric constituents' transportation in the upper troposphere and lower stratosphere (UTLS) and the variability of the Asian Monsoon Anticyclone (AMA). The Asian Monsoon Anticyclone (AMA) variability on different time scales has been proved to have significant effect on the UTLS transport process. In our previous research, the seasonal and intra-seasonal variation has been investigated. Here by using MERRA2 reanalysis data, we present some results for better understanding the impact from interannual variability on the mechanism of UTLS transport process.

## 1. Introduction

The Asian Monsoon Anticyclone (AMA) (also known as the South Asian or Tibetan Anticyclone) is an essential component governing the onset, maintenance and variability of the Asian monsoon. The recent discovery of an ATAL (Asian Tropopause Aerosol Layer) from recent satellite observations (Fig. 1), has sparked very active research work on the composition ( $H_2O$ , aerosols, and chemical species), and relationship of the ATAL to the AMA, near surface aerosols and climate change [Vernier, 2011, 2015; Pan, 2016; Yu, 2017].

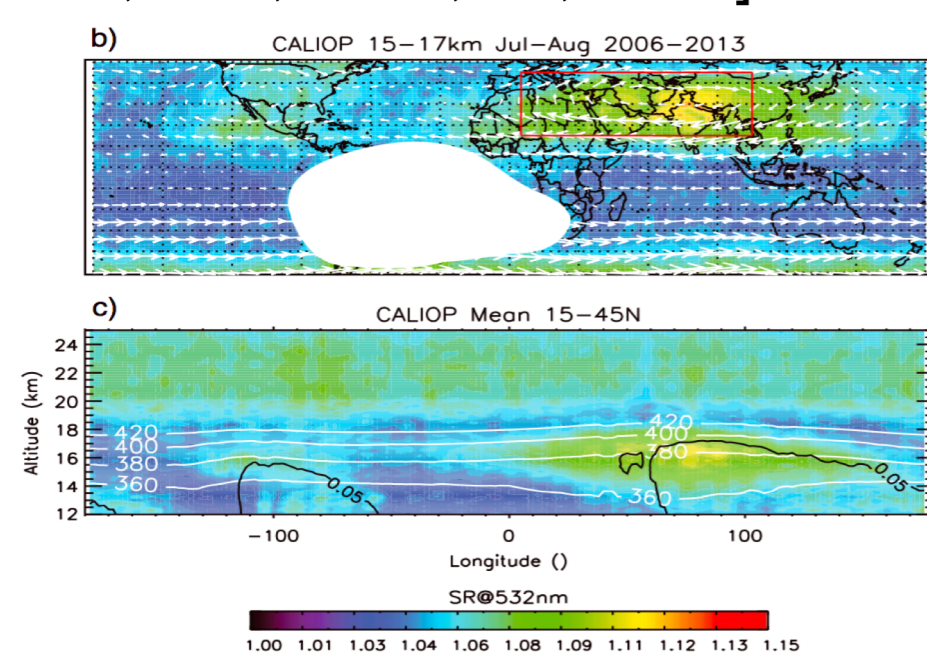


Fig. 1. The ATAL based on CALIOP LIDAR observation. (from Vernier et al., 2015)

In our previous work [Lau, 2018], we have found strong seasonal and intra-seasonal variations of the ATAL, involving transport of surface pollutants over Asian monsoon regions in the form of a planetary scale "Double-Stem-Chimney-Cloud" (DSCC), centered over the Himalayas Gangetic Plain (HGP) over India and the Sichuan Basin (SB) over China (Fig. 2). Here we use MERRA2 reanalysis data, which include aerosol data assimilation, to investigate the interannual variability the ATAL, in connection with variations of the DSCC and associated UTLS transport process.

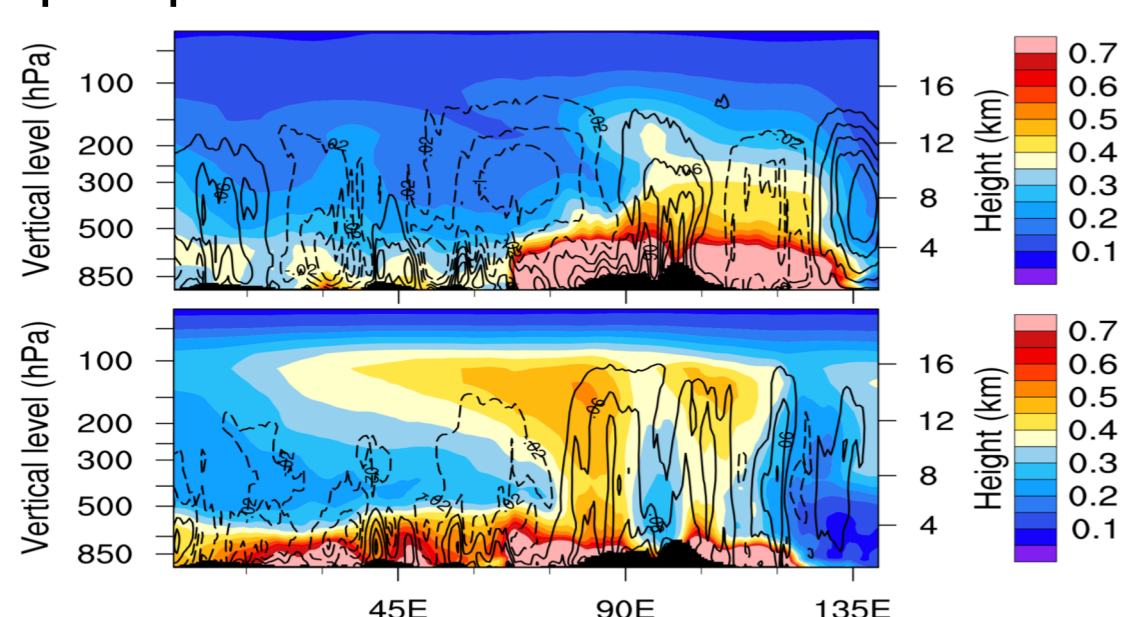


Fig. 2. The vertical profile of Carbonaceous Aerosol (CA), showing the DSCC during pre- and peak monsoon periods.

## 2. Methodology

A robust increasing trend can be seen during the data period (Fig. 3b). 2001-2006 are named as 'Early Part Years' (EP), and 2009-2015 are named as 'Late Part Years' (LP). We then detrended the rainfall time series, and we defined strong vs. weak monsoon years based on the detrended time series (Fig. 3c). Four strong monsoon years (2007, 2010, 2011 and 2013; denoted as "SM") and three weak monsoon years (2002, 2014 and 2015; denoted as "WM") were identified.

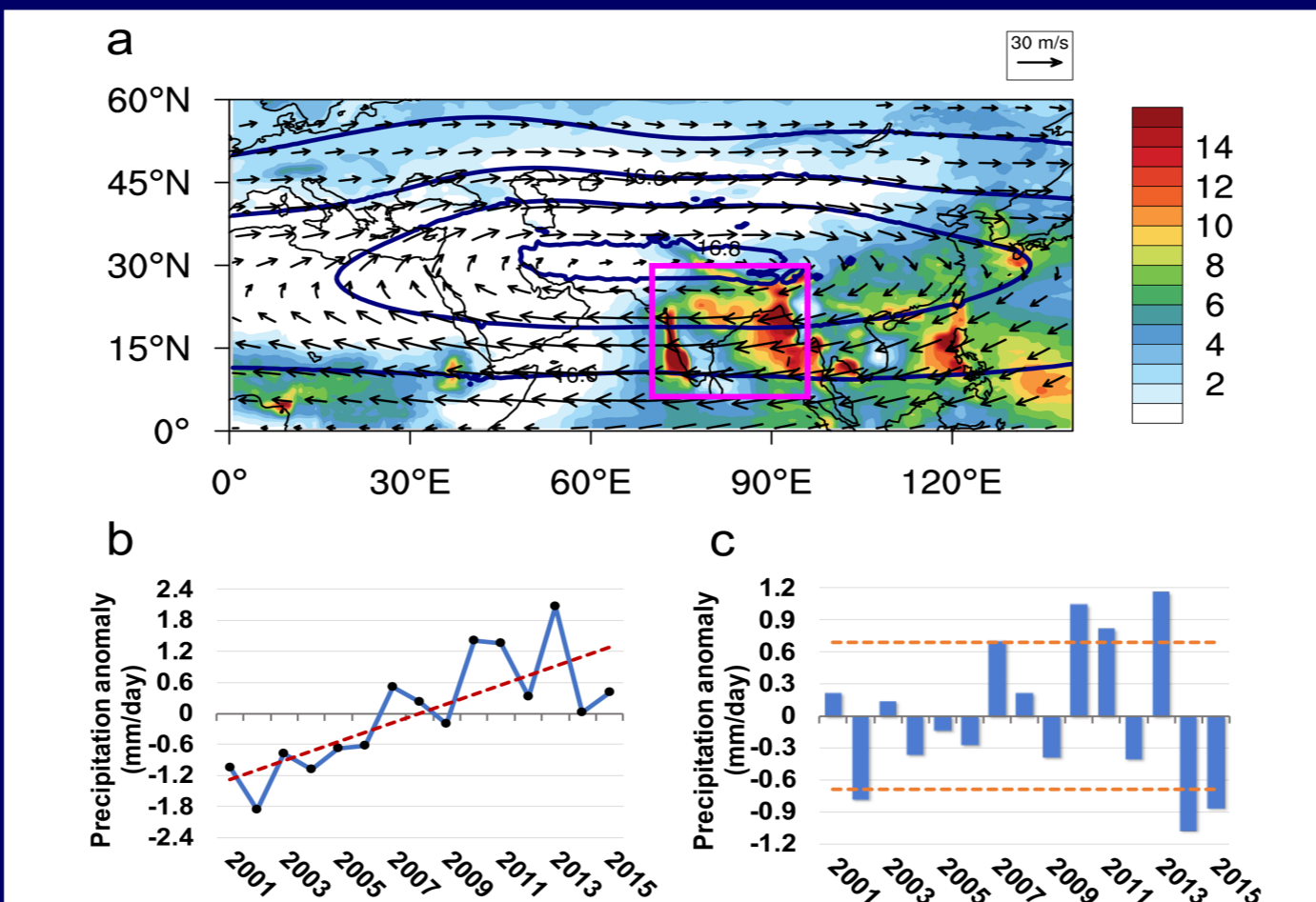


Fig. 3. Climatological mean ASM features associated with the AMA showing (a) the spatial distribution of winds (arrows, in  $ms^{-1}$ ), geopotential height at 100 hPa (solid contours, in km) and rainfall (colored background, in  $mm\ day^{-1}$ ) during July–August of 2001–2015. The pink box (5–30 N, 70 N–95 E) outlines the domain selected for calculating the precipitation intensity. (b) Time series of the precipitation anomaly from 2001 to 2015 (with the trend line in red). (c) The detrended distribution (with standard deviations in orange).

Composite mean distributions of monsoon meteorology, as well as aerosol loading transport, and ATAL variability were carried out for SM and WM, EP and LP respectively, based on the detrended data. Henceforth, the term "anomaly" in the following parts refers to the difference between SM and WM or LP and EP composites (SM minus WM, or LP minus EP).

## 3. Results

During SM years, the CO concentration is generally increased in the ATAL (Fig. 4a), consistent with the enhanced advection by the strengthened easterlies at the southern flank of the AMA. The large reduction in CO near the surface over east Asia may be related to the quenching of emission sources by increased precipitation over this region. For CA, the pattern of anomalies is similar to the pattern of CO, reduction in CA in the monsoon region (west of 70 E) is likely due to stronger precipitation washout during SM. Likewise, during SM, severely suppressed dust is found near the surface up to the mid-troposphere in the stem over the HGP (60–100 E), associated with washout by the increased precipitation (Fig. 4c).

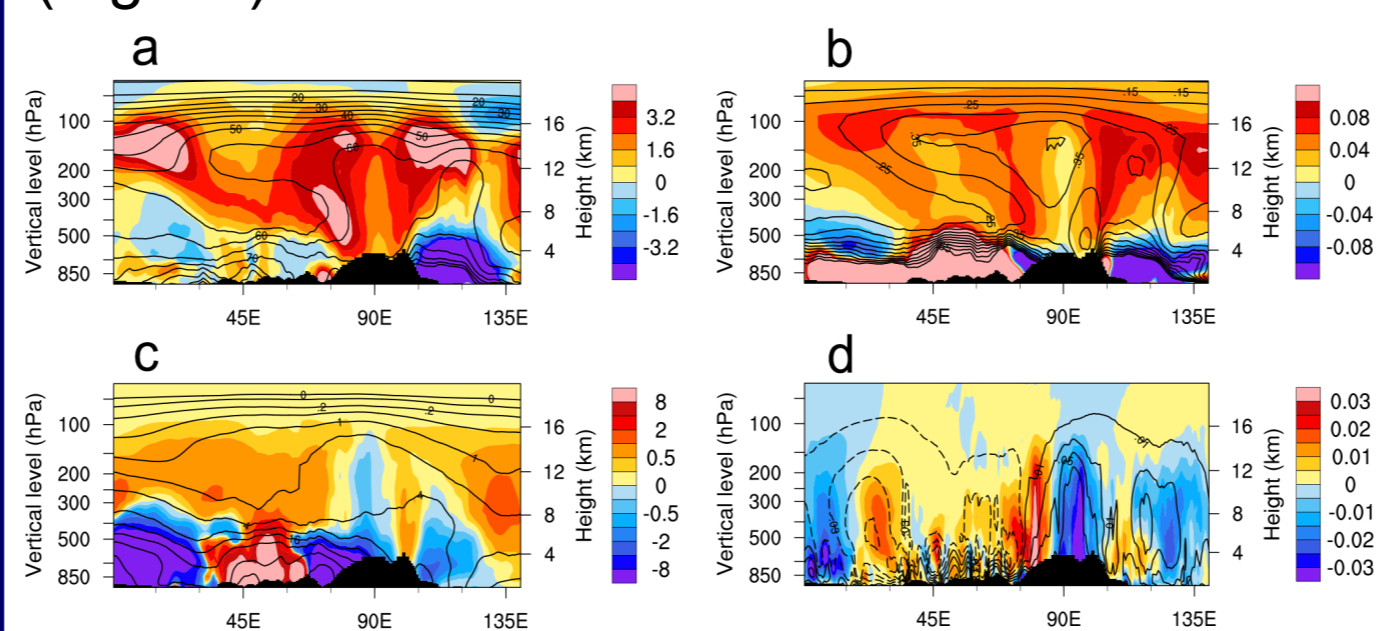


Fig. 4. Longitude–height cross sections (0–140 E) of (a) CO (ppbv), (b) CA (ppbm), (c) Dust (ppbm) and (d) vertical motion ( $Pa\ s^{-1}$ ) anomalies between strong and weak monsoon years ("strong" minus "weak") averaged over the southern portion of the AMA (25–35 N) during July–August, superimposed with the climatological mean of weak monsoon years (black contours). For vertical motions in (d), solid (dashed) contours indicate ascent (descent).

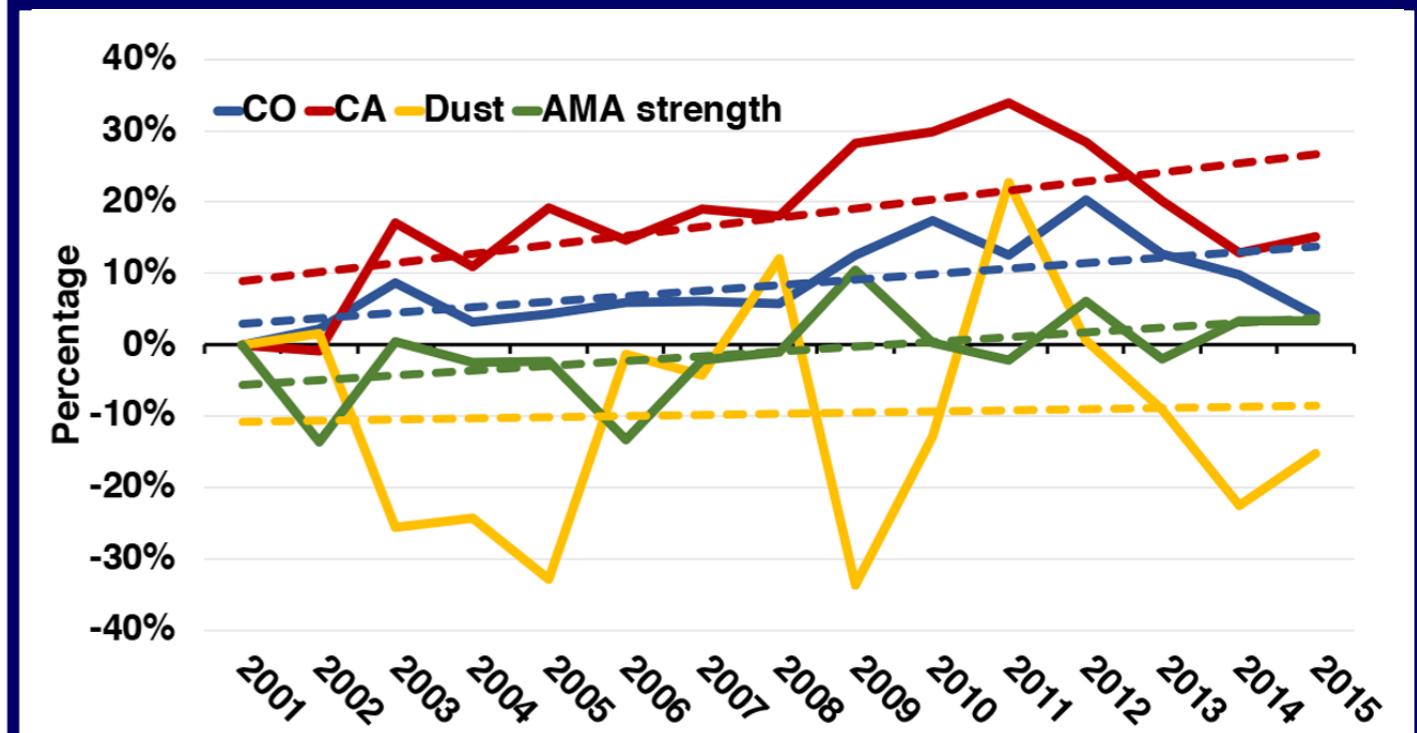


Fig. 5. Time series of CO, CA, dust and AMA strength anomalies relative to the first year during 2001–2015. The loading of CO, CA and dust is area-averaged over the selected region (that is, 25–35 N, 60–120 E). The AMA strength is calculated from the percentage difference in zonal wind averaged between 30 and 40 N minus zonal wind averaged between 10 and 20 N along the sector 60–120 E.

Clearly, CO and CA in the ATAL show significant increasing trends during 2001–2015, at a rate of +7.8% and +12.7% per, respectively. A similar trend of CO is also seen in the results from MLS observation. This could be attributed to the strengthening of the SASM during 2001–2015.

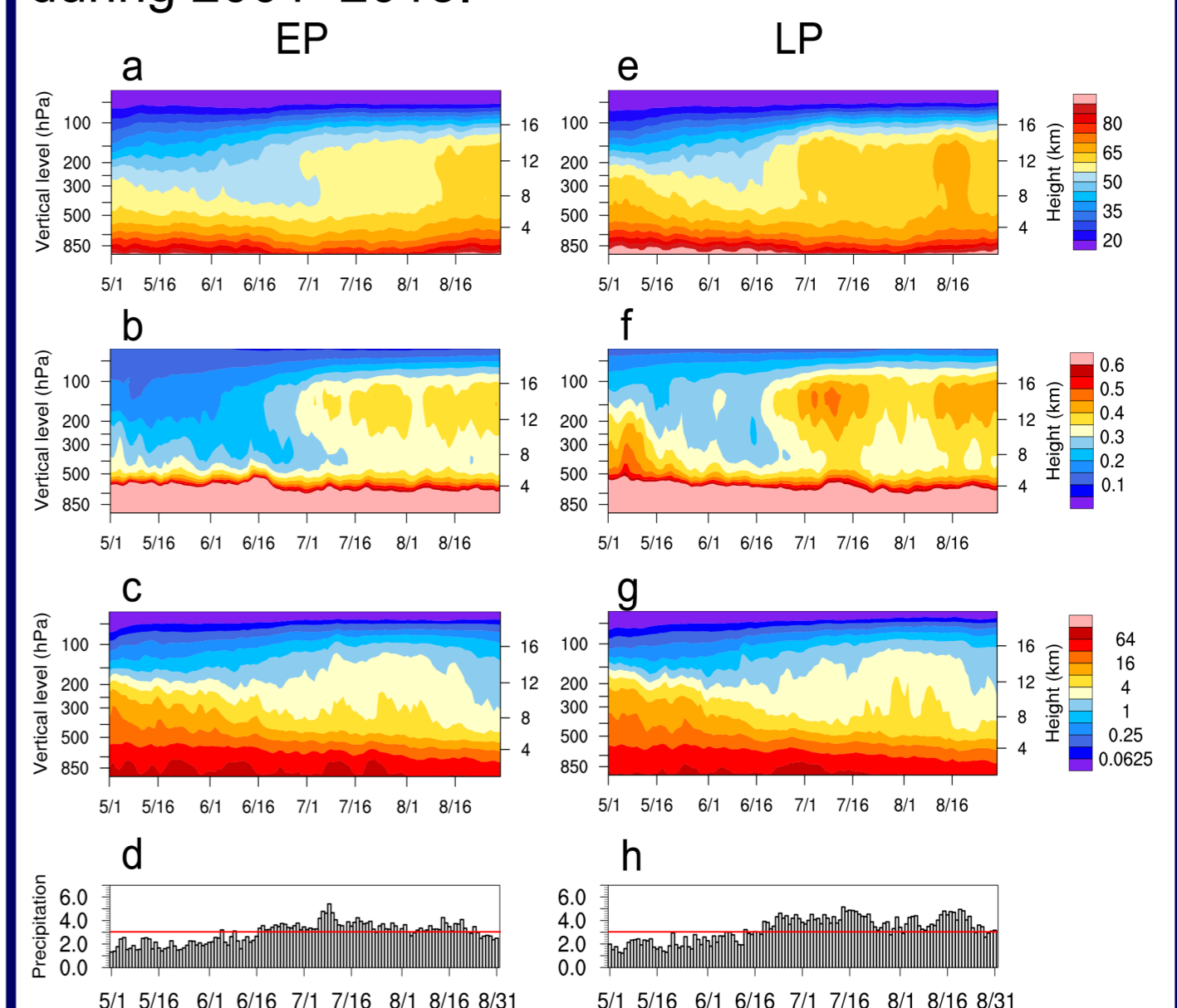


Fig. 6. Time–height cross sections showing daily variations in (a) CO (ppbv), (c) CA (ppbm), (e) dust (ppbm) and (g) precipitation ( $mm\ day^{-1}$ ) during early part years over the DSCC stem regions (25–35 N, 65–115 E). Panels (b), (d), (f) and (h) are the same as (a), (c), (e) and (g) but for late part years. Red lines in (g) and (h) show the reference value of precipitation intensity ( $3mm\ day^{-1}$ ).

During LP, monsoon precipitation is enhanced compared to EP from June through August (Fig. 6d, h). The onset of the monsoon, as characterized by an abrupt rise in CO to above 200 hPa reaching the ATAL, occurs earlier in LP (around 16 June) compared to EP (around 1 July). Likewise for CA, features such as the earlier onset, the increased ATAL concentration (above 200 hPa) and the longer residence time during LP are also pronounced.

## 5. Reference

- Vernier, J. P., L. W. Thomason, and J. Kar (2011), *Geo. Res. Lett.*, 38(7), L07804.
- Vernier, J. P., et al. (2015), *J. Geophys. Res.*, 120(4), 1608.
- Pan, L. L., et al. (2016), *J. Geophys. Res.*, 121(23), 14159.
- Yu, P., et al. (2017), *Proc. Nat. Aca. Sci.*, 114(27), 6972.
- Lau, W. K. M., C. Yuan, Z. Li (2018), *Sci. Rep.*, 8(1): 3960.